Set-membership localization and tracking of autonomous underwater vehicles

A. Caiti[a], A. Garulli[b], F. Livide[b], D. Prattichizzo[b]

[a]*ISME - Interuniv. Ctr. Integr. Sys. Marine Env., c/o DSEA, Univ. of Pisa, v. Diotisalvi2, Pisa, Italy; caiti@dsea.unipi.it*
[b]*DII - Dip. Ing. Inform., Univ. of Siena, v. Roma 56, Siena, Italy; e-mail: garulli@dii.unisi.it, prattichizzo@ing.unisi.it*

Summary

Algorithms are presented for localization and tracking of Autonomous Underwater Vehicles (AUVs) from acoustic time-of-flight measurements received by a field of surface floating buoys. The algorithms assume that measurements and AUV dynamics uncertainties are unknown but bounded, with known bounds, and produce as output the set in a 3-D space of admissible AUV positions. The algorithms are taylored for a shallow water situation, and account for realistic variations of the sound speed profile in sea water. The algorithms have been validated by simulations in which uncertainty models have been obtained from field data at sea. Localization performance of the algorithm are shown comparable with those previously reported in the literature by other approaches who assume knowledge of the statistics of measurement uncertainties. Tracking performance is shown worse than that of Extended Kalman Filter (EKF) when uncertainties are unbiased. In presence of non-zero mean disturbances (as currents, tides, etc.), the set-membership tracking algorithm outperforms EKF.

1. Introduction

Recent years have witnessed an impressive growth in the technology for undersea exploration. Remotely Operated Vehicles (ROVs) are today a well-established technology routinely used in the off-shore industry. Autonomous Underwater Vehicles (AUVs) are still more research topics than commercial products; however, they held the promise of being the next significative step in ocean exploration, allowing for operations that are presently not possible from surface ships or by ROVs. One of the problems that prevents commercial applications of AUVs is vehicle localization. The availability of (D)GPS systems on board of surface platforms has increased the demands on AUVs navigation accuracy. Inertial Navigation Systems (INS) cannot maintain the requested accuracy over the interval of operation of the system, and are highly expensive. The general problem of localization of autonomous vehicles has received much attention in the robotic literature [3, 6, 10, 11, 17]; however, the peculiarities of the underwater environment and of AUV missions prevent the simple transposition of available techniques for land or aerial vehicles, and require careful study of the implications of each chosen methodology for the underwater system performance [4, 16, 18]. There are several navigation systems currently employed by AUVs researchers. The main non-acoustic approach consist in installing on the AUV a GPS receiver, an INS and a Doppler Velocity Log (DVL); the vehicle navigates with the INS/DVL system, but periodically comes to surface to receive the GPS signal to recalibrate its absolute positioning [19]. The acoustic approaches can be subdivided in the Long and Short Base-Line systems (LBL/SBL). In both cases the vehicle position is determined on the basis of the acoustic returns detected by a set of receivers. In the LBL case, acoustic transponders are deployed on the seafloor around the perimeter of the area of operation. In SBL systems, a ship follows the AUV at short range with a high-frequency directional emitter. All these methods have merits and drawbacks. Augmented INS requires the installation of sophisticated sensors, and are vehicle-specific. LBL systems requires long time for deployement and calibration. SBL systems needs a ship to follow the vehicle; in this case, the vehicle is not really autonomous, but just untethered.

A simpler alternative to LBL/SBL systems has been recently investigated, consisting in installing acoustic receivers/emitters on surface freely floating buoys; on the buoys are installed also GPS receivers, and radio connection among themselves. The vehicle is located through simple time-of-flight measurements of acoustic pings from each buoy, with one of the buoys acting as a master station, i.e. collecting the information from the other buoys and determining the absolute position of the vehicles. Alternatively, each buoy emits at regular time intervals a ping with the coded information of its GPS position. The vehicle listen for the pings, and again from time-of-flight measurements determines its absolute position. In this second alternative, the floating buoys system has the ambition of becoming a true underwater GPS system, affordable, easy to deploy and recover, autonomous during its time of operation. The localization and tracking performance of such a system has been recently investigated by several authors [2, 5, 7, 13, 14]; in most of the cases, the algorithm analyzed have considered measurements affected by Gaussian-distributed noise, and have determined the resulting localization uncertainties through Monte Carlo analysis or nonlinear transformation techniques [5]. In this paper, a different approach is proposed and investigated, based on the assumption that measurements and modeling errors are unknown but bounded, with known worst case bounds. Tools from set-membership estimation theory [12] are employed to determine the admissible region in space in which the vehicle is located. Though the algorithm can be easily generalized to the deep water case, our discussion and implementation refers only to the shallow water case (water depth less than 500 m), which is the most interesting from the point of view of AUV applications, and the most challenging due to the presence of multipath effects. Two algorithms have been implemented, one for localization and one for tracking. The tracking algorithm relies on the localization algorithm to obtain point-wise measurements, and on a simple and general vehicle kinematic model. The performance of the algorithms has been tested in simulation, considering buoys dislocation similar to those employed in [5, 14] to allow comparison of results. The error measurement characteristics have been taken from field experiments at sea [13-15] to obtain a realistic evaluation of the approach. The results show that, in the localization case, the spatial distribution of uncertainty is similar to that obtained by methods that rely on the Gaussian assumption. In the tracking case, the set-membership approach has a performance which is worse than that of the Extended Kalman Filter (EKF) when errors are not polarized; however, when realistic disturbances are considered, as currents of unknown but bounded magnitude, the proposed algorithm has perfomance and robustness clearly superior to those of the EKF.

The paper is organized as follows: in the next section the problem is formally stated, and the methodological set-membership approach is described for both localization and tracking; in section 3 the localization algorithm is described; in section 4 a Monte Carlo analysis of performance of the localization algorithm is presented; in section 5 the tracking algorithm is introduced; in section 6 simulation results are presented, with results obtained with the proposed algorithm and with EKF; finally some conclusions are given.

2. Problem statement and the set-membership approach

Let us consider the situation in which n buoys are placed in arbitrary positions on the sea surface over an area of interest. An absolute earth reference system (x, y, z) is assumed, with z=0 on the water surface, and the z-axis pointing upward from the sea surface. Each buoy position $(x_i(t), y_i(t), 0)$ is assumed known. In practice, any buoy position will be known at D-GPS accuracy; however, the uncertainty in the position can be treated as an additional uncertainty in the buoy measurement. It is assumed that the AUV transmits at regular pre-specified time intervals a coded acoustic ping, which is received by each buoy. The symmetric situation, in which the buoys transmits a ping at known time instants, can be treated in a similar way. The ping coding serve the purpose of transmitting the information on the current AUV depth, and, in the tracking case, of the vehicle velocities. The low-level signal processing is not considered here. It is assumed that the received signals are suitably processed so that, after reception of each acoustic ping, the i-th buoy has available, at time t_k, the measurement $s_i(t_k)$ of the one-way travel time of the emitted ping from the AUV. Each measurement is affected by an unknown but bounded uncertainty $e_i(t_k)$, i.e.:

$$\begin{aligned} &s_i(t_k) = \tilde{s}_i(t_k) + e_i(t_k), \\ &|e_i(t_k)| \le E_i \quad \forall k,\ i = 1, \cdots, n \end{aligned} \tag{1}$$

being $\tilde{s}_i$ the measurement when no

uncertainties are present, and E a known bound on the worst-case uncertainty, in which all the uncertainties (noisy signals, D-GPS accuracy, buoy motion between transmission and reception, etc.) are concentrated. Each measurement is radio transmitted to a central station, together with each buoy D-GPS position, and the central station task is to provide the estimate of the absolute position of the vehicle. The sound speed $c(x,y,z)$ in the area of interest is assumed known. Though the algorithm can deal with the general case, in the following of the paper sound speed varies only with depth in the area of interest, i.e. $c(x,y,z)=c(z)$. Acoustic propagation is modeled with ray path theory [9] including multipath effects. Note that, for the purpose of the algorithm, only the acoustic ray paths need to be computed. The source and receivers are taken as omnidirectional. Propagation along the sea surface boundary has not been considered, since these rays are very much attenuated and scattered by wave motion and bubbles. Each ray reaching the i-th buoy with angle $\bar{q}(x_i,y_i,0)$ with respect to the plane (x,y) will move along a path such to respect the Snell's law at every point (x,y,z) of the path,:

$$\frac{\cos(q(x,y,z)}{c(z)}=\frac{\cos(\bar{q}(x_i,y_i,0)}{c(0)} \tag{2}$$

At each time t_k, the measurement of the i-th buoy defines a region $S_i(t_k)$ of the admissible space B_0 in which the vehicle is positioned. The space B_0 is bounded by the sea surface and the sea bottom (which may include varying bathymetry), and by the defined extension of the area of interest; The buoys are located inside B_0. Merging the information from all the available buoys, the vehicle must belong to the region $V(t_k)$ given by:

$$V(t_k)=B_0\cap\left(\bigcap_{i=1}^{n}S_i(t_k)\right) \tag{3}$$

The region $V(t_k)$ may have a complex geometrical shape, making it unfeasible its exact computation. The objective of the localization algorithm is to determine an approximation of $V(t_k)$ in terms of a box $B(t_k)\supseteq V(t_k)$. Boxes are convenient geometrical objects to use, since for their computation linear programming tools can be employed. The algorithm determines the box P of smallest volume containing the set V.

The tracking algorithm relies on a dynamic model of the AUV. Referring to Figure (1), the following kinematic model has been considered:

$$\begin{aligned}\dot{x}&=u\cdot\cos(j)-v\cdot sin(j)+w_x\\ \dot{y}&=u\cdot sin(j)+v\cdot\cos(j)+w_y\\ \dot{z}&=0\\ \dot{f}&=r+w_j\end{aligned} \tag{4}$$

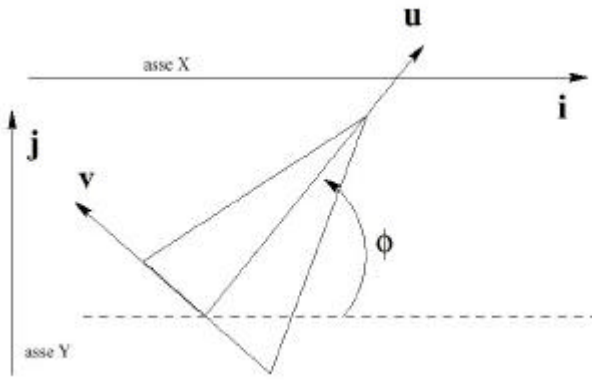

Figure 1: reference axis for the system in equation (4)

In equation (4), u,v and r are the surge, sway and yaw velocities of the AUV, that will be considered as known input. The terms w_h are the model uncertainties (including input uncertainties). The use of this planar model implies that, in the tracking case, the vehicle is equipped with depth and DVL sensors. The set-membership tracking algorithm will rely on a discretization in time of the system in equation (4). The general approach is here briefly described. Let $\mathbf{x}(k)$ be the state of the dynamic system of interest, and $\mathbf{y}(k)$ the vector of available measurements. Let the dynamic equations be expressed in compact form as:

$$\begin{aligned}\mathbf{x}(k+1)&=\mathbf{f}(\mathbf{x}(k),k)+\mathbf{w}(k)\\ \mathbf{y}(k)&=\mathbf{h}(\mathbf{x}(k),k)+\mathbf{m}(k)\end{aligned} \tag{5}$$

where the uncertainty vectors **w** and **m** are unknown but bounded, with worst case bounds known, i.e. $\|\mathbf{w}\|_\infty\le E_w,\|\mathbf{m}\|_\infty\le E_m$; the admissible set to which the generic vector **z** belongs is indicated in the following as *Z*. Let the initial conditions be specified as:

$$\mathbf{x}(1)\in X(1/0) \tag{6}$$

being $X(1/0)$ a known set. The objective of the tracking algorithm is to recursively compute the set of states $X(k/k)$ (state estimate) and $X(k+1/k)$ (state prediction) compatible with the information available at time k. Let $C_\infty(k)$ the set of system states compatible with the measurement at time k:

$$C_\infty(k) = \left\{ \mathbf{x} : \left\| \mathbf{y}(k) - \mathbf{h}(\mathbf{x}(k), k) \right\|_\infty \le \mathrm{E}_m \right\} \qquad (7)$$

The sets $X(k/k)$ and $X(k+1/k)$ are then determined by the following recursive relations:

$$\begin{aligned} X(k/k) &= X(k/k-1) \cap C_\infty(k) \\ X(k+1/k) &= \mathbf{f}(X(k/k), k) + B_w \end{aligned} \qquad (8)$$

where B_w is a box whose size depends on E_w. The geometrical shape of the sets $X(k/k)$ and $X(k+1/k)$ may be fairly complex, so they will be approximated by bounding boxes $B(k/k)$ and $B(k+1/k)$ such that:

$$\begin{aligned} &B(1/0) \supseteq X(1|0) \\ &B(k/k) \supseteq B(k/k-1) \cap C_\infty(k) \\ &B(k+1/k) \supseteq \mathbf{f}(B(k/k), k) + B_w \end{aligned} \qquad (9)$$

and such to be the optimal (smallest) boxes to include the sets $X(k/k)$ and $X(k+1/k)$.

3. The localization algorithm

For the sake of clarity, the set-membership localization algorithm will be described for the case of constant sound speed with depth, i.e. $c(z) = c$. The results reported in the following section, however, will cover both the constant and the variable sound speed cases. With constant sound speed, the distance of the veichle from the *i*-th buoy is computed from the measurement equation (1) as:

$$\begin{aligned} d_i(t_k) &= \frac{s_i(t_k)}{c} = \frac{\tilde{s}_i(t_k) + e_i(t_k)}{c} = \\ &= \tilde{d}_i(t_k) + e_i(t_k), \\ \left| e_i(t_k) \right| &\le \frac{E_i}{c} = F_i, \qquad i = 1, \cdots, n \end{aligned} \qquad (10)$$

Let us freeze the time t_k. The set of vehicle positions compatible with the measurement d_i is a spherical cap L_i of center $\mathbf{c}_i = (x_i, y_i, 0)$ (the buoy position) and of internal and external radii $R_{1i} = d_i - F_i$ and $R_{2i} = d_i + F_i$ respectively. The set V of vehicle positions compatible with the measurements from all the buoys is obtained by substituting the terms S_i with L_i in equation (3). In order to find the smallest box approximation of V the following procedure is employed. At first, the intersections of L_i and L_j for all the possible couples $i, j, i \neq j$ are considered. Let $\mathbf{x}$ be a point in the earth absolute reference system. Consider the change of coordinates such that $\mathbf{x} = \mathrm{A}\,\mathbf{v} + \mathbf{c}_i$, where the first column of the matrix A is given by the unitary vector $\mathbf{x}_c = \dfrac{\mathbf{c}_i - \mathbf{c}_j}{\left\| \mathbf{c}_i - \mathbf{c}_j \right\|}$ and the other two columns can be taken as any vectors orthonormal to $\mathbf{x}_c$; in particular, we have chosen the new z axis equal to that of the absolute reference system (an admissible choice, since $\mathbf{x}_c$ lies on the sea surface plane) . The new coordinate system has the x axis aligned with the vector $\mathbf{x}_c$ joining the centers of the two spherical caps, and origin in one of the two centers. Since the intersection problem has cylindrical symmetry with respect to the $\mathbf{x}_c$-oriented axis, the two caps can be projected on the plane generated by $\mathbf{x}_c$ and by one of the other two axis. The projection on this plane gives origin to two circular anuli H_i and H_j. The rectangle with minimal area containing the intersection of H_i and H_j is identified by determining the max and min x and y coordinates over the set $H_i \cap H_j$. This can be done by simple enumeration of the intersection points among the two anuli, and of each anulus with the $\mathbf{x}_c$-oriented axis. The rectangle thus obtained (see Figure 2) can be rotated along the $\mathbf{x}_c$-oriented axis to generate a cylinder which includes the admissible region, of radius $r = y_{\max}$ and of height $h = x_{\max} - x_{\min}$; this cylinder is bounded by a box B defined by the constraints:

$$\begin{aligned} &x_{\max} \ge v_1 \ge x_{\min} \\ &r \ge v_2 \ge -r \\ &r \ge v_3 \ge -r \end{aligned} \qquad (11)$$

being $\mathbf{v} = (v_1, v_2, v_3) \in B$. The transformation $\mathbf{x} = \mathrm{A}\,\mathbf{v} + \mathbf{c}_i$ can be inverted, and equation (11) can be written in the earth absolute reference frame as a set of six linear inequalities in the form:

$$\mathrm{M}_{ij}\,\mathbf{x} \le \mathbf{b}_{ij}, \qquad \mathrm{M}_{ij} \in \Re^{6\times 3} \qquad (12)$$

Let $B_k, k = 1, \cdots, n(n-1)/2$ be the set of all boxes determined by considering all the possible pairs L_i, L_j; recall that B_0 is the whole region of space where the AUV can be positioned.

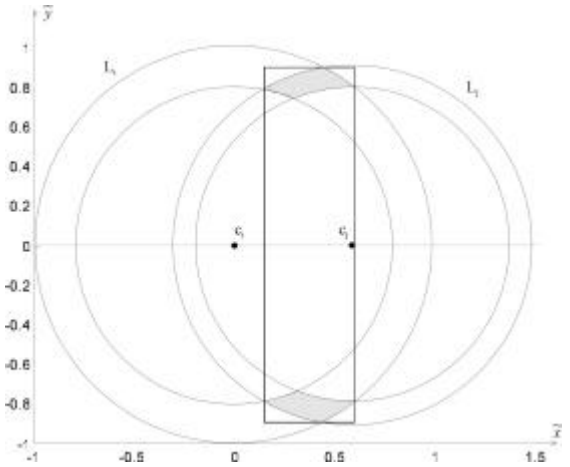

Figure 2: intersection between two spherical caps L_i, L_j (planar view); the admissible regions for the vehicles are the gray shaded regions. The rectangle represents the box of minimal volume containing the admissible region. The coordinate system has an axis oriented along the line through the buoys *i, j* (the centers of the spherical caps).

Each box is defined by a set of constraints:

$$\mathrm{M}_k \mathbf{x} = \mathbf{b}_k, \qquad k = 1, \cdots, n(n-1)/2 \qquad (13)$$

The final localization box *B* will be given by the box of minimal volume including the intersection of the boxes $B_k, k = 0, \cdots, n(n-1)/2$; in a given coordinate frame, the box containing such intersection is simply found by solving six linear programming problems, that is, being $\mathbf{x} = (x, y, z)$ a point in the given coordinate system, by solving:

$$\begin{aligned} &\min(x), \max(x), \min(y), \max(y), \min(z), \max(z) \\ &\text{subject to constraints:} \\ &\mathrm{M}_k \mathbf{x} = \mathbf{b}_k \qquad k = 1, \cdots, n(n-1)/2 \end{aligned} \qquad (14)$$

Care must be taken since it is not true that a box of minimal volume in a given coordinate system has minimal volume for any coordinate system. So the following iterative procedure is started:

a) solve (14) in the absolute coordinate system obtaining a box P; set $B \leftarrow P$;

b) for every buoy *i*, $i = 1, \cdots, k$, compute a coordinate transformation setting the *x* axis along the direction joining the center of *B* with the buoy position, then solve (14) in the new coordinate system obtaining a box *P*; if *volume(P)<volume(B)* set $B \leftarrow P$;

c) if *volume(B)* has not changed during the last step, exit with the result *B*; otherwise, go to step b).

This procedure is sub-optimal, since it does not check the condition of minimal volume along all possible coordinate transformations. However, it does check the minimality conditions over a set of privileged directions, that are those joining the buoy positions with the best estimate currently available of the AUV position. The procedure is computationally feasible as long as the number of linear constraints is of the order of 500 (i.e., the number of buoys is kept below 15) standard available programs can efficiently perform the computation. Our implementation relies on the package MOSEK to solve the constrained linear programming problems.

4. Localization algorithm: performance analysis

Performance analysis of the set-membership localization algorithm is now reported. An admissible region of 30×30 Km in the (x, y) plane is considered, with water depth of 150 m. Three buoys are considered, placed as vertex of a triangle of 16 Km side. The admissible region has been gridded in the (x, y) plane at 1 Km spacing. The depth of the vehicle has been kept at 75 m at any point of the grid. For each point of the grid, 10 different measurements realizations have been generated, and the localization algorithm applied. The average worst case localization error over the set of the 10 realization is reported for each point. The worst case localization error is computed as the semidiagonal of the computed bounding box *B* which includes the admissible region *V*. The measurements realization have been obtained first assuming a uniformly distributed measurement error e_i (see equation (10)) within the interval $[-100, 100]$m, independent identicallly distributed (i.i.d.) for each buoy; in a second case, Gaussian distributed measurement error has been assumed (again, i.i.d. for each buoy), with zero mean and standard deviation $s = 33$ m. In both cases, the algorithm assumes the knowledge of the worst case error $F_i = 100$ m ($3s$ in the Gaussian case). Note also that a 33 m standard deviation, assuming a constant sound speed of 1500 m/s, corresponds to a standard deviation of 22 ms in the (one way) time of arrival measurement error: this figure is derived from the field data in [15], where the *two-way* travel time standard deviation was reported between 30 and 60 ms. Figure 3 shows the results obtained with uniformly distributed measurement errors. Figure 4 reports the results obtained with Gaussian distributed measurement noise.

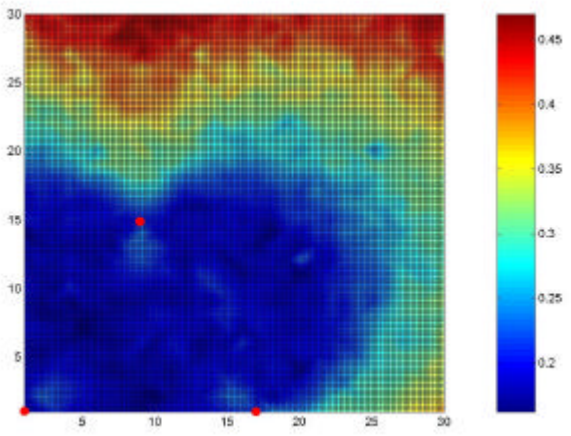

Figure 3: Color-coded average worst case error over the admissible region in the case of uniformly distributed measurement error, constant sound speed profile. The error chromatic scale is in Km. Buoy locations are the red circles. Scales on the *x* and *y* axis are in Km

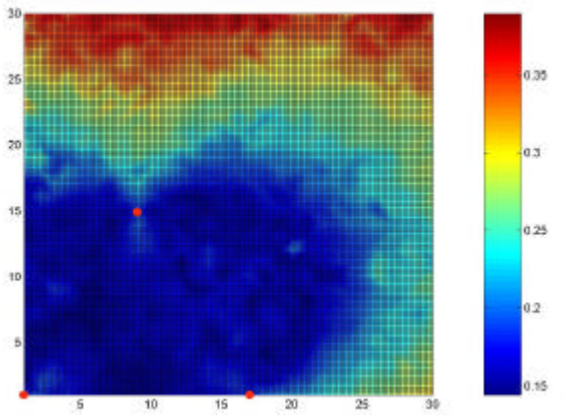

Figure 4: Color-coded average worst case error over the admissible region in the case of Gaussian distributed measurement error, constant sound speed profile. The error chromatic scale is in Km. Buoy locations are the red circles. Scales on the *x* and *y* axis are in Km.

It has to be emphasized that here the worst case localization error has been shown, i.e. the errors reported are not the magnitude of the distance of the true position from the box center, but the magnitude of the box semidiagonal, i.e., the worst case possible error if the measurements do respect the assumed bounds. When comparing the results obtained by other authors in similar configurations [5, 15] the error distribution in space is similar, and the worst case errors here reported are only slightly higher than those of the cited works. Taking into account that in those works the true position was used to compute the average error, one can conclude that the algorithms have similar performance. Note that localization in the Gaussian case with the set-membership algorithm causes higher worst case errors, as it should be expected, but not a significative degradation of performance.

For the variable sound speed case, the sound speed profile has been taken as in Figure 5 ("summer conditions"). The measurement error e_i has been taken in a first case as uniformly distributed over the interval $[-75,75]$ ms, and i.i.d. for every buoy; in a second case the error has been taken as Gaussian i.i.d. for every buoy, with standard deviation $s = 25$ ms. In both cases, the localization algorithm is given information of the worst case measurement error $E_i = 75\,\text{ms}\ \forall i$. Gridding and pseudo Monte Carlo analysis have been performed as in the constant sound speed case. Results are reported in Figures 6 and 7. The results show that summer conditions cause a degradation of performance in the localization algorithm at long ranges from the buoys

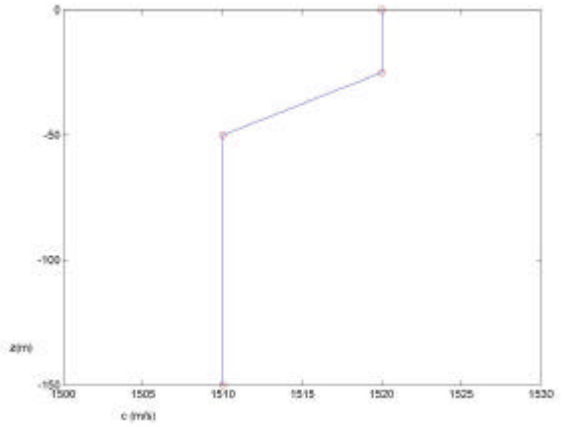

Figure 5: sound speed profile used to generate the data of Figures 6-7. The profile is typical of summer conditions in shallow water.Water depth is 150m.

5. The tracking algorithm

The set-membership tracking algorithm for the AUV kinematic model of equation (4) is now described. The system state is composed by the

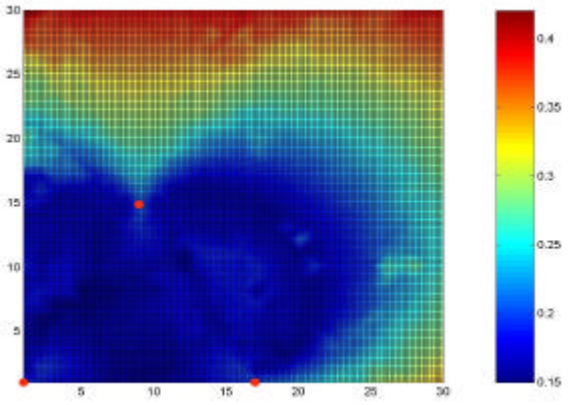

Figure 6: Color-coded average worst case error over the admissible region in the case of uniformly distributed measurement error, summer conditions. The error chromatic scale is in Km. Buoy locations are the red circles. Scales on the *x* and *y* axis are in Km

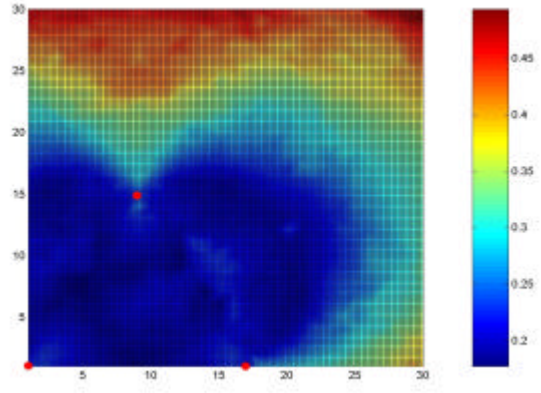

Figure 7: Color-coded average worst case error over the admissible region in the case of Gaussian distributed measurement error, summer conditions. The error chromatic scale is in Km. Buoy locations are the red circles. Scales on the *x* and *y* axis are in Km

variables x, y and j, i.e. planar dynamics are considered, with no AUV movement along the depth axis *z*. It is assumed that the system inputs u, v and r are exactly known; the model and input uncertainties w_x, w_y, w_j are unknown but limited by known bounds W_x, W_y, W_j. Available measurements are the (x, y) position of the AUV, as obtained by the localization algorithm, and the measurement of j, obtained from gyro on board the AUV, affected by an unknown but bounded uncertainty e_j, $|e_j| \le E_j$ .Let us set Δt as sampling interval for the acquisition of new measurements. As described through equations (5-9), the tracking algorithm is based on the intersection of the sets generated by the system predictions and by the available measurements, computed on the basis of the known worst case modeling and measurement errors. To compute predictions for the system in equation (4), let us consider first the dynamic equation of the state variable j, which is independent from the other states. Let us suppose that at the $(k-1)$-th sampling interval it is available the information on the compact set $I(\Phi_{1,k-1}, \Phi_{2,k-1})$ to which $j(k-1)$ belongs: $\Phi_{1,k-1} \le j(k-1) \le \Phi_{2,k-1}$. Then the state $j(k)$ must belong to the following set:

$$I(\Phi_{1,k}, \Phi_{2,k}) = I(\Phi_{1,k-1} - E_f \Delta t, \Phi_{2,k-1} + E_f \Delta t) + \int_{(k-1)\Delta t}^{k\Delta t} r\, dt \quad (15)$$

At any time $t, (k-1)\Delta t \le t < k\Delta t$, $j(t)$ must belong to the set:

$$I(\Phi_{1,t}, \Phi_{2,t}) = I(\Phi_{1,k-1} - E_f \Delta t, \Phi_{2,k-1} + E_f \Delta t) + \int_{(k-1)\Delta t}^{t} r\, dt \quad (16)$$

The goal of the analysis is now to bound the admissible evolution of the states *x* and *y* within the sampling interval. In order to reach the goal, a bound on the maximum and minimum time derivative of the states must be determined. Consider the following quantities related to the variable *x*:

$$\begin{aligned} d_1(t) &= u(t)\cdot\cos(\Phi_{1,t}) - v(t)\cdot sin(\Phi_{1,t}) + W_x \\ d_2(t) &= u(t)\cdot\cos(\Phi_{2,t}) - v(t)\cdot sin(\Phi_{2,t}) + W_x \\ d_3(t) &= u(t)\cdot\cos\left(-\text{arctg}\left(\frac{v(t)}{u(t)}\right)\right) + \\ &\quad - v(t)\cdot sin\left(-\text{arctg}\left(\frac{v(t)}{u(t)}\right)\right) + E_x \end{aligned} \quad (17)$$

which are the derivatives of *x* computed at the boundaries of the admissible interval of j, for the j that maximizes the *x* derivative computed by setting $\partial\dot{x}/\partial j = -u\,\text{sen}(j) - v\cos(j) = 0$. At any instant *t* the maximum derivative of *x* is given by:

$$\dot{x}_{\max}(t) = \max \dot{x}(t) = \max(d_1(t), d_2(t), d_3(t)) \quad (18)$$

subject to the constraint:

$$-\text{arctg}\left(\frac{v(t)}{u(t)}\right) + n\cdot p \in I(\Phi_{1,t}, \Phi_{2,t}) \quad (19)$$

Expressions similar to those of equations (17-19) can be derived for the minimum time derivative of x and y. Consider the compact set $I(X_{1,k-1}, X_{2,k-1})$, $X_{1,k-1} \le x(k-1) \le X_{2,k-1}$. Then $x(k)$ and $y(k)$ are bounded by:

$$\begin{aligned} X_{1,k} &= X_{1,k-1} + \\ &+ \int_{(k-1)\Delta t}^{k\Delta t} (\dot{x}_{\min}(t) - W_x)dt \le x(k) \le X_{2,k-1} + \\ &+ \int_{(k-1)\Delta t}^{k\Delta t} (\dot{x}_{\max}(t) + W_x)dt = X_{2,k} \\ Y_{1,k} &= Y_{1,k-1} + \\ &+ \int_{(k-1)\Delta t}^{k\Delta t} (\dot{y}_{\min}(t) - W_y)dt \le y(k) \le Y_{2,k-1} + \\ &+ \int_{(k-1)\Delta t}^{k\Delta t} (\dot{y}_{\max}(t) + W_y)dt = Y \end{aligned} \quad (20)$$

Equations (15) and (20) allows to iteratively generate predictions for the admissible regions of the state space in which the system must lie. Since j is independent from the (x,y) position, consider the set $B(k/k-1)$ as the predicted box in the (x,y) space bounding the admissibile system positions. Let $B(k)$ be the bounding box on the system position obtained from the acoustic measurements at time k with the localization algorithm. The estimated system state will be bounded by the box $B(k/k)$ of minimal volume and such that:

$$B(k/k) \supseteq B(k) \cap B(k/k-1) \quad (21)$$

A similar set-membership estimate can be derived for j. The computation of minimal volume bounding boxes has been implemented with linear programming methods. No computational difficulties have been encountered, since in this case the constraints are intersections of planes.

6. Tracking algorithm: performance analysis

The set-membership tracking algorithm has been compared with the classic Extended Kalman Filter (EKF) tracking. Two cases are presented, both assuming constant sound speed in water. In the first, the process and measurement errors are generated by uniform distributions with zero mean. The set-membership algorithm has knowledge of the bounds on the distribution intervals, and the EKF has been initialized with a diagonal covariance matrix, where the elements of the diagonal has been taken so that the resulting ellipsoid covers the 95% of the volume of the uncertainty boxes. The second case is similar to the first, but for the presence of a constant bias in some of the process uncertainties. In the first case, three buoys are employed for the range measurements, in the same configuration illustrated in the localization case. The error bounds are: $W_x = W_y = 0.2$ m/s, $W_j = 0.02$ rad/s. The range measurements are i.i.d with measurement errors $F_i \le 100$ m for every buoy i at any sample instant. The gyro errors are also i.i.d., with uniform probability distribution and bound $E_j \le 0.0175$ rad. The sampling interval Δt is 10 s. Vehicle depth has been held constant at 75 m. In the simulations, the complete system dynamics have been taken into account, using the models described in [8]. A bow-tie path of 10 Km lenght inside the admissible region has been implemented as path to be tracked. Figure 8 reports the errors between the estimated positions and the true ones, for both the EKF and the set-membership algorithm. The box center has been taken as estimated position of the set-membership algorithm. Figure 10 reports the 99% confidence interval of the EKF and the worst case bounds from the set-membership algorithm.

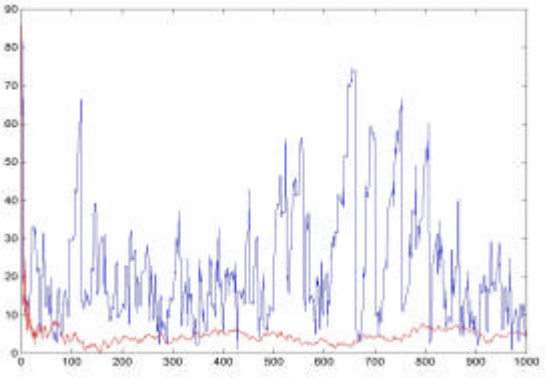

Figure 8: Error as a function of sampling instant along the path for both tracking algorithms. X-scale is in sampling intervals, Y-scale is in meters. The blue line is the error of the set-membership tracking algorithm, the red line is the error of the EKF tracking.

Clearly the EKF has a better performance with respect to the set-membership tracking algorithm; moreover, the EKF estimation of the error (Figure 9) is consistent with the effective error, so that the EKF covariance matrix can be employed as a check of the tracking accuracy. The worst case error bounds as estimated by the set-membership algorithm are also consistent with the effective errors. In the second the uncertainties w_x, w_y, wh are generated independently from a uniform distribution with interval $[-0.12, 0.2]$m/s. The average model uncertainties mimic the presence of a very modest constant current of 0.06 m/s. The set-membership algorithm still has the a priori knowledge of a worst case error of magnitude 0.2 m/s, and the EKF covariance matrix is initialized as in the previous case. In Figure 10 the tracking errors are reported; in Figure 11 the 99% confidence of the EKF tracking and the worst case bounds on the set-membership error are reported.

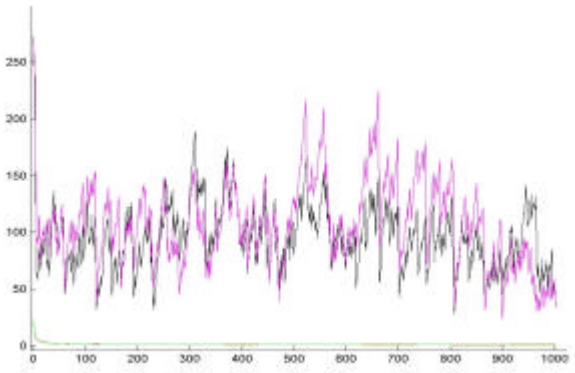

Figure 9: Worst case error bounds for the set-membership tracking (black, *x* axis; violet, *y* axis) and 99% confidence intervals estimated by the EKF through the covariance matrix (green, *x* axis; red, *y* axis - they overlap in such a way to be almost undistinguishable). X-axis in the figure is in sampling intervals, Y-axis is in meters

It is well known that, in presence of unmodelled biases, the Kalman Filter performs poorly, and this case is no exception, as it can be seen in Figure 10. The point here is that, as shown in Figure 11, the EKF has no knowledge of its poor performance: the estimated confidence intervals from the covariance matrix are very small, indicating a very precise tracking estimate (which is obviously not the case). The set-membership tracking algorithm, on the contrary, has by construction always control on the worst case error. Constant bias of unknown magnitude can be included in the EKF setting,

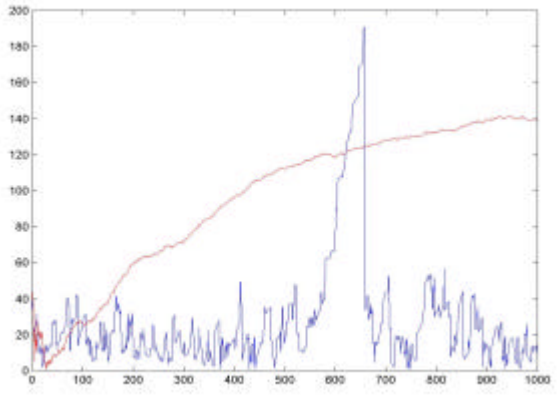

Figure 10: Error as a function of sampling instant along the path for both tracking algorithms. X-scale is in sampling intervals, Y-scale is in meters. The blue line is the error of the set-membership tracking algorithm, the red line is the error of the EKF tracking.

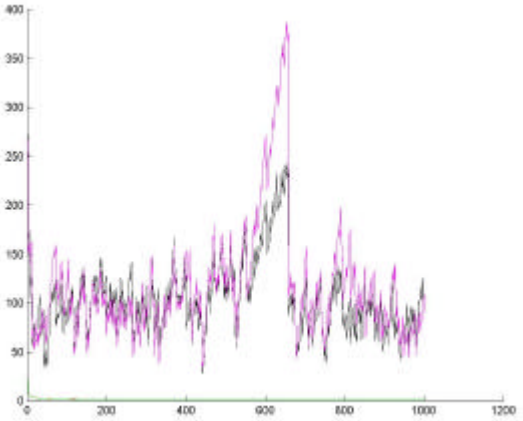

Figure 11: Worst case error bounds for the set-membership tracking (black, *x* axis; violet, *y* axis) and 99% confidence intervals estimated by the EKF through the covariance matrix (green, *x* axis; red, *y* axis both included in the interval between 0 and 10 m/s, but for the initialization transient). X-axis in the figure is in sampling intervals, Y-axis is in meters

improving the tracking performance. On the other hand, time-varying non-zero mean disturbances will always give origin to EKF tracking errors as those reported here. Ocean currents and tides are both space and time varying [1], so the EKF performance is bound to be degraded in realistic oceanic conditions.

7. Discussion and conclusions

Localization and tracking algorithms for AUV with measurements from a sparse field of acoustic buoys have been presented. The algorithms are based on set-membership estimation theory, and produce as output the region in space to which the AUV must belong, on the basis of the worst case

bounds on the measurement and process errors. No statistical assumptions on the disturbances are made. Being a worst-case scenario, the set-membership localization produces slightly higher nominal errors than other methods, but with the same spatial distribution. The set-membership tracking performance has been compared with the EKF. As long as no bias are present in the process or measurement uncertainties, the EKF tracking is more accurate, and is able to correctly estimate also its own confidence interval. When realistic ocean conditions are considered, not only the EKF performance degrades, but also its confidence interval estimation falls apart. On the contrary, the set-membership algorithm is insensitive to biases, and it is always able, to correctly estimate its range of accuracy.

Acknowledgements

Supported by MURST, Project "Self-localization algorithms for air and maritime vehicles with guaranteed uncertainty bounds"

References

[1] A.Alvarez, A.Caiti: A genetic algorithm for underwater vehicles route planning in ocean environments with complex space-time variability, Proc. IFAC Conf. Control Applications in Marine Systems, Glasgow, 2001

[2] C.Bechaz., H.Thomas: GIB system: the underwater GPS solution, Proc. 5th Europ. Conf. Underwater Acoustics, Lyon, 2000.

[3]J.Borenstein, H.R.Everett, L.Feng: Navigating Mobile Robots: Sensors and Techniques, A.K.Peters, Ltd., Wellesley, MA, 1995.

[4]A.Caiti: Seafloor exploration with parametric sonar systems: current issues and challenges for underwater vehicles, Proc. IEEE Conf. Control Applications, Trieste, 1998.

[5]L.Collin, S.Azou, K.Yao, G.Burel: On spatial uncertainty in a surface long base-line positioning system, Proc. 5th Europ. Conf. Underwater Acoustics, Lyon, 2000.

[6]A.Garulli, A.Vicino, Uncertainty sets for dynamic localization of mobile robots, Proc. 38-th IEEE Conference on Decision and Control, Phoenix, 1998, pp. 1488-1493.

[7]J.P.Hermand, et al.: Geoacoustic inversion with drifting buoys: EnVerse 1997-98 experiment, in Caiti, Hermand, Jesus and Porter (Eds.): Experimental acoustic inversion methods for exploration of the shallow water environment, Kluwer Acad. Publ., Dordrecht, 2000.

[8]G.Indiveri: Modeling and identification of underwater robotic systems, Ph.D. thesis (in English), DIST, University of Genova, 1998.

[9]F.Jensen, W.Kuperman, M.B.Porter, H.Schmidt: Computational Ocean Acoustics, Am. Inst. Physics, New York, 1994

[10]J.J.Leonard, H.F.Durrant-Whyte: Mobile robot localization by tracking geometric beacons, IEEE Trans. Robotics and Automation, **7**(3), 1995.

[11]T.S.Levitt, D.T.Lawton: Qualitative Navigation for Mobile Robots, Artificial Intelligence, **44**(3), 1990, pp.305-360.

[12]M.Milanese, A.Vicino: Information based complexity and nonparametric worst-case system identification, Journal of Complexity, **9**, 1993, pp. 427-446.

[13]L.Mozzone, S.Bongi: Localization and fusion of echoes with deployable multistatic active sonar: evaluation of feasibility using experimental data, Proc. 4th Europ. Conf. Underwater Acoustics, Rome, 1998.

[14]L.Mozzone, P.Lorenzelli, A.Caiti, S.Bongi: Target motion analysis with multiple distributed acoustic sensors, Proc. 5th Europ. Conf. Underwater Acoustics, Lyon, 2000.

[15]L.Mozzone, P.Lorenzelli, A.Caiti, S.Bongi: Acoustic localization of marine crafts with multistatic deployable sonars, Proc. 5th IFAC Conf. Manoeuvring Control Marine Crafts, Aalborg, 2000.

[16]J.S.Stambaugh, R.B.Thibault: Navigation Requirements For Autonomous Underwater Vehicles, Navigation, **39** (1), 1993.

[17]K.T.Sutherland, W.B.Thompson: Localizing in unstructured environments: dealing with the errors, IEEE Transactions on Robotics and Automation, **10**(6), 1994, pp.740-754.

[18]S.T.Tuohy, J.J.Leonard, J.G.Bellingham, N.M.Patrikalakis, C.Chryssostomidis: Map based navigation for autonomous underwater vehicles, Int. J. Offshore Polar Eng. **6**(1), 1996.

[19]X.Yun, et al.: Testing and Evaluation of an Integrated GPS/INS System for Small AUV Navigation, IEEE J. Oceanic Eng., **24** (3), 1999.